Screening for Profitable Retrofit Options of Chemical Processes: a New Method

Eric Uerdingen, Ulrich Fischer, and Konrad Hungerbühler
Safety & Environmental Technology Group, Laboratory of Technical Chemistry,
Swiss Federal Institute of Technology (ETH), CH-8093 Zurich, Switzerland

Rafiqul Gani
Technical University of Denmark, Dept. of Chemical Engineering, CAPEC, DK-2800 Lyngby, Denmark

A new systematic methodology for screening retrofit options to improve the economics of a continuous chemical process is organized in three stages: 1. base case analysis; 2. generation of retrofit options; and 3. rough economic evaluation of the retrofit options. In stage 1, the flowsheet of a process, based on the steady-state mass and energy balances of a representative process operating state (base case), is decomposed into open and cycle component path flows with their corresponding flow rates. In the path flow assessment, variable process costs are then allocated to these component flows through two economic indicators representing raw material consumption, and energy and waste cost. Additional physico-chemical path flow indicators characterizing the degree of nonideality of the process are also calculated. In stage 2, the results of the path flow assessment are used to identify possible retrofit options with the help of recommended retrofit actions. In stage 3, the impact of retrofit options on variable costs of the base case is estimated and discussed in terms of its technical feasibility. This method has been applied to the hydro-dealkylation process for the toluene production. Several promising retrofit options were identified through this method. The results demonstrate how the new method supports the systematic identification of economically beneficial retrofit options for chemical processes.

Introduction

Competition on the chemical market has increased during the past decades. Therefore, to be still competitive, most existing production processes need constant improvement through retrofitting. The goals of retrofitting a chemical process can be manifold, that is, to increase production capacity, to reduce operating costs and, thus, to increase profitability, to implement a more efficient technology, to increase product quality, or to reduce emissions to the environment.

Different methodologies have been used for evaluating the retrofit potential of a chemical process with regard to one of these objectives. For example, Rapoport et al. (1994) presented a strategy using heuristic rules for the generation of retrofit options, while Jaksland et al. (1995) presented a thermodynamic insights based synthesis method for generating process alternatives applicable to new processes, as well as existing processes. Tjoe and Linnhoff (1986) applied pinch analysis—previously introduced by Linnhoff and Flower (1978)—to retrofit design, and, among many others, Ciric and Floudas (1989) used algorithmic approaches such as mixed integer nonlinear programming (MINLP). Also, combinations of these methods have been applied, for example, Kovac and Glavic (1995) combined thermodynamic and algorithmic methods for retrofitting complex and energy intensive processes.

A number of retrofit studies concentrated on single aspects of a chemical process, that is, Kürüm et al. (1997) focused on entrainer selection, Dantus and High (1996) on waste minimization or process integration, Guntern et al. (1998) on optimizing the reactor, Ciric and Floudas (1989) on heat-exchange networks, Fraser and Hallale (2000) on mass-exchange networks, and van der Helm and High (1996) on waste

Correspondence concerning this article should be addressed to U. Fischer.

minimization. Only a few studies have aimed at revealing retrofit opportunities of an entire chemical process. Fisher et al. (1987) and Rapoport et al. (1994) presented methodologies enabling a systematic analysis of process flowsheets with regard to their retrofit options. The method presented by Rapoport et al. (1994) uses rules based on heuristics and is organized in a hierarchical procedure, in which the improvement of the existing flowsheet, the selection and optimization of additional operation units, and the optimized design of heat integration are covered in this sequence.

The most elaborated retrofit methodology to date was presented by Fisher et al. (1987). Their method is thought as a tool for developing and also screening retrofit opportunities. It is again organized as a hierarchical procedure with the following sequence: (a) use an operating cost diagram for the existing process to identify the incentive for raw material and energy savings, (b) determine the incentive for completely replacing the existing plant, (c) screen the process options, and find the best flowsheet if the existing plant is to be replaced completely, (d) modify the existing equipment sizes for the existing flowsheet or a structural alternative, and (e) refine the retrofit calculations. One element in the analysis of the existing process is that, in the operating cost diagram, all the significant operating costs are attached to stream arrows on the current process flowsheet.

In this article a new methodology for identifying and screening the retrofit potential of a chemical process is presented. This method is also based on a detailed economic analysis of the process under investigation by decomposing it into component path flows and assigning the associated costs. Besides the economic parameters, additional indicators are also used to characterize the degree of nonideality in a process. These indicators can then be used to identify retrofit opportunities, to generate process options, and to rank these due to their economic improvement potential. The new method has been applied to the hydro-dealkylation process for the production of toluene (HDA) as a case study and the results obtained demonstrate how the systematic framework of the new methodology supports the identification of economically beneficial retrofit options for chemical processes.

New Methodology

The first stage of the new methodology (see Figure 1) is the *path flow decomposition* procedure (Stage 1), which decomposes a process flowsheet into a set of flow trajectories (path flows) of each component in the process. In the next stage these component path flows are assessed independently with various economic and physicochemical performance indicators and are subsequently ranked according to an economic performance measure (*path flow assessment*; Stage 2). Finally, retrofit options—in terms of either process parameters to be optimized or structural changes in the process design to be realized—are identified on the basis of the path flow assessment results, are ranked according to their economic impact potential, and are finally discussed with regard to their technical feasibility (*identification of retrofit options*; Stage 3).

The screening method is applicable to continuously operating production processes and requires the knowledge of the main component mass balances, as well as an energy balance

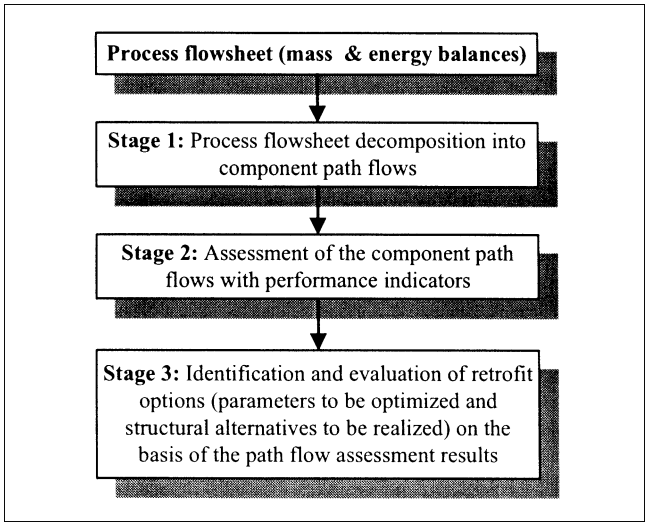

Figure 1. Principle of the new screening method with the stages path flow decomposition, path flow assessment, and identification of retrofit options.

at a characteristic steady-state operating point. Furthermore, economic data for raw materials, utilities, waste disposal, and products are required. Moreover, the process boundaries have to be clearly defined, as complex connections between different processes are often encountered at a production site.

Stage 1: path flow decomposition

The flowsheet of the investigated process is represented as a directed process graph that consists of a set of vertices (unit operations or sequence of unit operations) and edges (streams). The flow decomposition technique, derived from the graph optimization theory, transforms all process stream flows into path flows of the various components involved in the process. A process without recycles can be decomposed into open path flows. An open path flow of a single component consists of a trajectory from a supply vertex (input/generation by chemical reaction) to a demand vertex (output/consumption by chemical reaction). If recycling occurs in the process, the path flow decomposition technique additionally yields cycle (closed) path flows that begin and end in the same vertex. The decomposition procedure, as shown in Figure 2, consists of four steps.

Step 1-1. If recycling occurs, all cycles in the investigated process have to be identified before starting the path flow decomposition procedure. Sargent and Westerberg (1964) and, later, Tarjan (1972) introduced a general algorithm for the systematic identification of cycles (strongly connected components in a digraph—a visualization technique that is used to represent chemical process flowsheets). The algorithm consists in backtracking paths in a process graph until an already visited vertex is encountered for the second time —this procedure is repeated until all cycles are determined. All vertices participating in these cycles can thus be identified and formulated as a sub-graph of the complete process graph.

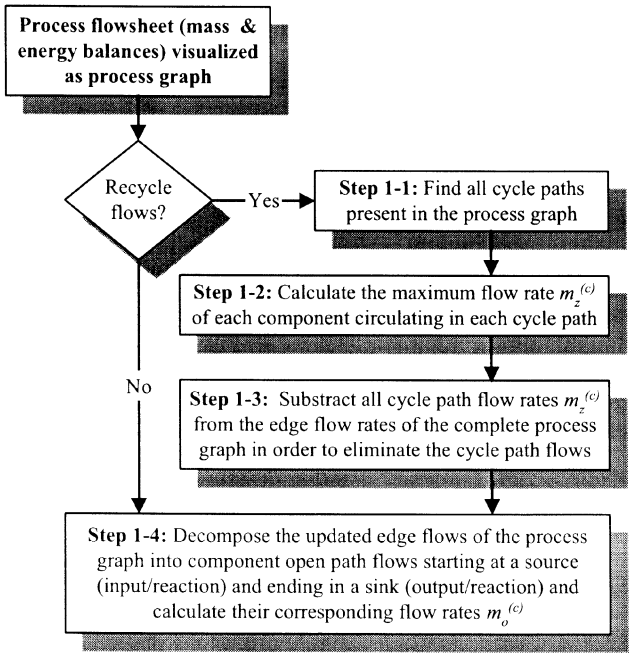

Figure 2. Principle of Stage 1 of the new method: path flow decomposition procedure.

Step 1-2. As illustrated in Figure 3, mass balance equations are then established for each vertex of all cycle paths and each component flowing in the cycles of the sub-graph

$$\sum_{a=1}^{EP} f_{i,a}^{(c)} - \sum_{b=1}^{EN} f_{b,i}^{(c)} = d_i^{(c)} - s_i^{(c)} \tag{1}$$

$$d_i^{(c)} = \sum_{op=1}^{OP} d_{i,op}^{(c)} + \sum_{or=1}^{OR} d_{i,or}^{(c)} \tag{2}$$

$$s_i^{(c)} = \sum_{ip=1}^{IP} S_{i,ip}^{(c)} + \sum_{ir=1}^{IR} S_{i,ir}^{(c)} \tag{3}$$

$$\forall i \in SG, \quad \forall c \in SC$$

where $f_{i,a}^{(c)}$ and $f_{b,i}^{(c)}$ represent the flow rates of component c in positively and negatively incident edges of vertex i, $s_{i,ip}^{(c)}$ and $s_{i,ir}^{(c)}$ are supply flow rates that either enter vertex i in a feed or are generated through reaction in i, $d_{i,op}^{(c)}$ and $d_{i,or}^{(c)}$ are demand flow rates that either leave vertex i in a process

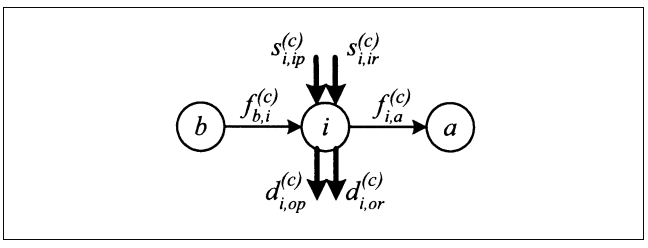

Figure 3. Mass balance at a single vertex *i*.
The corresponding equations are in Eqs. 1–3.

output flow or are eliminated through reaction in i, respectively, $s_i^{(c)}$ and $d_i^{(c)}$ represent the sum of all supply flow rates and all demand flow rates of component c at vertex i, EP and EN are the number of positively and negatively incident edges of i, OP and IP are the number of process output flows and process feed flows in i, OR and IR are the number of demand and supply flows involved in reactions, SG is the set of vertices of the sub-graph, and SC is the set of components flowing through the sub-graph.

Further, the linear mass balance equations of all vertices of the sub-graph, as given in Figure 3, can be represented in matrix notation

$$\bar{B}^{(c)}\vec{f}^{(c)} = \vec{d}^{(c)} - \vec{s}^{(c)} \tag{4}$$

where $\bar{B}^{(c)}$ denotes the edge-vertex incidence matrix that describes the aforementioned sub-graph from Step 1-1 and $\vec{f}^{(c)}$ represents the vector containing the mass-flow rates of a single component in each edge of the complete process graph. The vectors $\vec{d}^{(c)}$ and $\vec{s}^{(c)}$, finally, hold the total demand $d_i^{(c)}$ and supply $s_i^{(c)}$ mass-flow rates to each vertex of the sub-graph.

In order to calculate the mass flow of a component in each cycle the following optimization problem can be formulated

$$\max \sum_j y_j^{(c)} \tag{5}$$

$$\text{s.t. } \bar{B}^{(c)}\left[\text{diag}\left(f^{(c)}\right) y^{(c)}\right] = 0 \tag{6}$$

$$\forall y_j^{(c)} \in (0;1)$$

The vector $y^{(c)}$ contains mass-flow fractions $y_j^{(c)}$ of each flow rate in the vector $f^{(c)}$. The optimization problem simultaneously calculates for each cycle path the path flow rate for a given component such that the constraints defined in Eq. 6 are still fulfilled. Finally, these flow rates can then be determined with the maximized vector $y^{(c)}$ in the following manner

$$\bar{D}^{(c)}x^{(c)} = \text{diag}\left(f^{(c)}\right) y^{(c)} \tag{7}$$

where $\bar{D}^{(c)}$ represents the cycle-edge incidence matrix that attributes each edge of the sub-graph to one or more cycles. The vector $x^{(c)}$ contains the cycle path flow rates for all cycles and can be calculated by solving Eq. 7. Although this equation-system seems to be over-determined (more equations than cycles), it can be reduced to a linearly independent system of equations that contains the same number of equations as cycles in the sub-graph in which component c flows.

Step 1-3. Once the cycle path flow rates have been calculated for each component and cycle, they are subtracted from the complete process graph. This procedure eliminates all cycle flows and leaves only open path flows in the now updated process graph.

Step 1-4. In the next step, flow distribution factors are established at each vertex of the complete process graph updated in Step 1-3. For processes in which no recycling occurs, the flow decomposition procedure begins at this step. In process graphs with multiple supply and demand flows for one

component a procedure has to be defined for allocating a supply flow to the different demand flows. Therefore, the assumption is made that ideal mixing occurs in each vertex. Thus, it is assumed that each flow entering a vertex leaves the vertex via the different exit flows with a probability proportional to their mass-flow rates. The flow distribution factors are defined for all flows leaving a vertex i (see Figure 3), such as demand flows, and positively incident edges

$$F_i^{(c)} = \sum_{b=1}^{N} f_{b,i}^{(c)} + \sum_{ip=1}^{IP} s_{i,ip}^{(c)} + \sum_{ir=1}^{IR} s_{i,ir}^{(c)} \tag{8}$$

$$w_{i,op}^{(c)} = \frac{d_{i,op}^{(c)}}{F_i^{(c)}} \tag{9a}$$

$$w_{i,or}^{(c)} = \frac{d_{i,or}^{(c)}}{F_i^{(c)}} \tag{9b}$$

$$w_{i,a}^{(c)} = \frac{f_{i,a}^{(c)}}{F_i^{(c)}} \tag{9c}$$

In case $F_i^{(c)}$ is zero, all distribution factors in vertex i are automatically set to zero. The following six-step algorithm describes this procedure for component c:

(1) Select a supply flow $s_{i,ip}^{(c)}$ or $s_{i,ir}^{(c)}$ in vertex i.

(2) Choose either an edge $f_{i,a}^{(c)}$ or a demand flow ($d_{i,op}^{(c)}$ or $d_{i,or}^{(c)}$) leaving the vertex with component c. If a demand flow was chosen go to step 4, otherwise, continue.

(3) If an edge was chosen, follow the edge to the next vertex and repeat from step 2 at the new vertex.

(4) Check if all possible flow trajectories (open path flows) from the selected supply flow of component c to all demand flows of component c have been determined in the complete process graph. If yes, continue. Otherwise, go to step 2.

(5) Check if all supply flows have been selected. If not, select a new supply flow and repeat steps 1 to 4. Otherwise, continue.

(6) Calculate the corresponding flow rates for the entire open path flows determined through steps 1 to 5 by multiplication of the original supply flow rates with all distribution factors that occur along their various path flows.

After application of the flow decomposition procedure to all relevant components c, the complete process graph has been decomposed into open and cycle component path flows. The sum of all path flow rates flowing through any edge yields the original flow in that edge prior to flow decomposition.

Stage 2: path flow assessment

Cycle and open path flows are assessed with a set of indicators that quantitatively or qualitatively assess their performance within the process. The presented set of indicators is especially focused on maximizing economic efficiency. However, the modularity of the approach allows for additional indicators to be integrated for other retrofit goals. Figure 4 gives an overview of the assessment procedure. The different indicators are discussed in the following.

Material-value added (MVA). The *MVA*-indicator is only applicable to open component path flows leaving the process

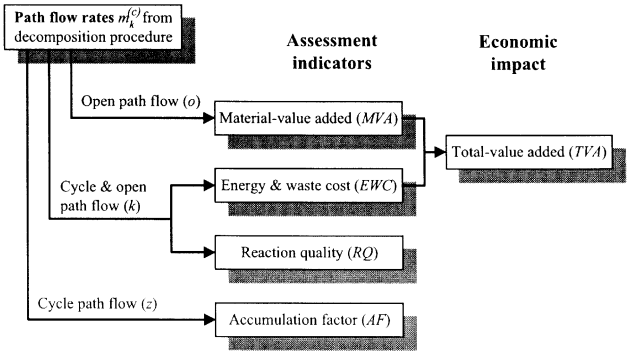

Figure 4. Overview of Stage 2 of the new method: component path flow assessment procedure.

boundaries in demand flows $d_{i,op}^{(c)}$ (see Figure 3) and calculates the difference between the value they represent outside the process boundaries and the costs in raw material consumption they caused (such as solvent: fuel credit in incineration − solvent purchase cost)

$$MVA_o^{(c)} = m_o^{(c)}\left(PP_o^{(c)} - PR_o^{(c)}\right) \tag{10}$$

where $m_o^{(c)}$, $PP_o^{(c)}$, and $PR_o^{(c)}$ represent the flow rate of component c in open path flow o, the specific value outside the process boundaries, and the purchase price, respectively. Negative *MVA*-values indicate undesired value losses and, hence, highlight potentials for improvement on economic efficiency. Equation 10 is used to calculate *MVA*-values for open path flows of components that are externally fed to the process via supply flows $s_{i,ip}^{(c)}$ (see Figure 3). The remaining open path flows necessarily originate in reaction supply flows $s_{i,ir}^{(c)}$ (Figure 3).

Before *MVA*-values can be calculated for these open path flows, *overall reaction equations* have to be formulated for the corresponding components starting from the process raw materials (only if multiple reaction steps are involved). In analogy to Eq. 10 the equivalent purchase value for a component generated in the process is determined by its raw material consumption calculated with the help of the raw materials' molecular weights $M^{(rm)}$, stoichiometric coefficients $\nu^{(rm)}$ from the overall reaction equation, and purchase prices $PR^{(rm)}$

$$MVA_o^{(c)} = m_o^{(c)}\left(PP_o^{(c)} - CA_o^{(c)}\left(\sum_{rm=1}^{RM} \frac{|\nu_o^{(rm)}| M_o^{(rm)}}{\nu_o^{(c)} M_o^{(c)}} PR_o^{(rm)}\right)\right) \tag{11}$$

where rm is the raw material index and RM is the total number of raw materials involved in the overall reaction equation. As multiple products are often generated in an overall reaction equation, it becomes necessary to allocate the raw material costs to the components flowing in the investigated open path flows. If at least one of the products of the overall reaction equation generates a value outside the process boundaries, the cost allocation factor $CA_o^{(c)}$ is calculated us-

ing the following convention

$$CA_o^{(c)} = \frac{PP_o^{(c)}}{\sum_{pd=1}^{PD} PP^{(pd)}} \tag{12}$$

where the superscript pd denotes a product and PD denotes the total number of products of the gross reaction equation. In case a product pd generates multiple specific values, $PP^{(pd)}$ represents the maximum specific value obtained. If no product generates a value outside the process boundaries, the allocation is based on the products' molecular weights

$$CA_o^{(c)} = \frac{M_o^{(c)}}{\sum_{pd=1}^{PD} M_o^{(pd)}} \tag{13}$$

Energy and waste cost (EWC). The EWC-indicator quantitatively allocates overall process costs related to utility consumption and waste treatment to a component path flow. The allocation deliberately neglects molecular interactions (such as heats of mixing) in mixed process streams and, therefore, idealizes the distribution of utility and waste treatment costs. The results indicate cost reduction potentials in each specific component path flow. Nevertheless, often only fractions of these potentials can be tapped by retrofit design depending on process constraints (such as safety, product quality, environmental regulations, thermodynamic constraints, and equipment constraints).

A unit-operation consists of one or more basic sub-operations (such as condenser: condensing and cooling). Before allocation, it becomes necessary to first attribute a fraction of each unit-operation's energy consumption to all of its sub-operations. If the exact contributions cannot be easily determined, a good estimate is sufficient for screening purposes. Moreover, each component path flow traversing a unit-operation is assigned to one or more of its sub-operations. This assignment depends on the influence that a given component path flow has on each sub-operation encountered along its path. In case that an investigated component path flow has no influence on a given sub-operation along its path the energy consumption of this sub-operation is not considered in the cost allocation. In the opposite case the sub-operation needs to be considered.

In case there is only a weak influence the decision has to be taken by the user if the sub-operation is to be considered or not. The allocation of process utility costs to a component path flow $EC_k^{(c)}$ is then handled in the following manner

$$EC_k^{(c)} = \sum_{u=1}^{U} PE_u Q_u \frac{m_k^{(c)} A_{u,k}^{(c)}(T_m, p_m)}{\sum_{uk=1}^{UK} m_{u,uk} A_{u,uk}(T_m, p_m)} \tag{14}$$

where u is the sub-operation index for all sub-operations considered for cost allocation along a component path flow k, U represents the total number of sub-operations considered for that path flow k, uk is the index of all component path flows involved in a given sub-operation u, UK represents the total number of component path flows involved in that sub-operation, and Q_u and PE_u represent the specific energy consumption and price of the utility needed for sub-operation u, respectively. Sub-operation-specific allocation factors A_u at mean temperatures T_m and pressures p_m (such as heating and cooling in a single phase: heat capacity of component) are also used in Eq. 14.

Waste treatment costs only concern open component path flows leaving the process boundaries to a waste treatment facility. Most often, waste treatment costs are already pre-allocated because the prices for waste treatment usually depend on the waste composition (such as Total Organic Carbon (TOC) content, total volume or mass, salt concentration, and heavy metal concentration). Therefore, waste treatment costs for components are defined according to mass, volume, concentration, or a combination of these and can be generalized by the following equation

$$WC_j^{(c)} = m_k^{(c)} \cdot \begin{Bmatrix} (\rho_j)^{-1} & WAV_j^{(c)} & \text{(volume allocation)} \\ & WAM_j^{(c)} & \text{(mass allocation)} \\ (V_j)^{-1} & WAC_j^{(c)} & \text{(allocation by concentration)} \end{Bmatrix} \tag{15}$$

where ρ_j and V_j represent the density and volumetric flow rate of the process stream j leaving the process boundaries, $WAV_j^{(c)}$ represents the volume-specific allocation factor for component c, $WAM_j^{(c)}$ represents the mass-specific allocation factor for component c, and $WAC_j^{(c)}$ represents the concentration-specific allocation factor for component c. The final EWC-indicator covers both energy and waste costs

$$EWC_k^{(c)} = EC_k^{(c)} + WC_k^{(c)} \tag{16}$$

Reaction Quality (RQ). The RQ-indicator qualitatively measures the effect of a component path flow k upon reactions that occur along its path. Positive RQ-values indicate a positive effect on overall plant productivity (defined as the total mole flow rate of the reactants required per total mole flow rate of the desired products produced), whereas negative values identify undesirably located component path flows in the process and thus highlight potential for cost savings through mass-flow reduction or rerouting of a path flow. The RQ-value of a path flow is calculated as the sum of its effects on reactive unit-operations along the path

$$RQ_k^{(c)} = \sum_{r=1}^{R} \sum_{rk=1}^{RK} \frac{\xi_{r,rk,k} E_{r,rk,k}^{(c)}}{\sum_{fp=1}^{FP} n^{(fp)}} \tag{17}$$

where $\xi_{r,rk,k}$ represents the extent of reaction rk, $n^{(fp)}$ represents the mole flow rate of a desired final product fp ($\{1, \ldots, FP\}$) of the process, r represents the index of reactive unit-operations ($\{1, \ldots, R\}$) along path flow k, and rk represents the index of all reactions $\{1, \ldots, RK\}$ in reactive unit-operation r affected by path flow k. The definition of the RQ-in-

dicator in Eq. 17 contains a parameter $E^{(c)}_{r,rk,k}$ that characterizes the effect of the component flowing in path flow k on each reaction involved in the path flow

$$E^{(c)}_{r,rk,k} = \begin{cases} +1, & \text{if component } c \text{ in } k \text{ affects reaction } rk \text{ such that the total productivity of the desired products } n^{(fp)} \text{ is favored} \\ 0, & \text{if component } c \text{ in } k \text{ has no effect on reaction } rk \text{ and the total productivity of the desired products } n^{(fp)} \text{ is unchanged} \\ -1, & \text{if component } c \text{ in } k \text{ affects reaction } rk \text{ such that the total productivity of the desired products } n^{(fp)} \text{ is inhibited} \end{cases} \quad (18)$$

The qualitative values of the effect-parameters $E^{(c)}_{r,rk,k}$ can be determined depending on the most relevant type of information available: kinetic information, plant experience, or thermodynamic data.

Accumulation Factor (AF). The *AF*-indicator rates the accumulative behavior in recycle flows and, therefore, only applies to component cycle path flows. A large accumulation factor often indicates unfavorable buildup in a cycle and can be caused by nonoptimal separation or too low reaction conversion. As cycle accumulation should typically be as low as technically feasible for obvious economic reasons, high *AF*-values can thus pinpoint potentials for cost reduction. High *AF*-values might be desired for valuable raw materials, solvents or auxiliaries.

The *AF*-indicator is calculated as the ratio of a component cycle path flow rate $m^{(c)}_z$ and the sum of all flows of that component leaving the cycle flow ($f^{(c)}_{i,a}$ and $d^{(c)}_{i,op}$) from any of its vertices i of the set of vertices CP in the cycle flow

$$AF^{(c)}_z = \frac{m^{(c)}_z}{\sum_{i=l}^{I} \left\{ \sum_{a=1}^{EP} f^{(c)}_{i,a} + \sum_{op=1}^{OP} d^{(c)}_{i,op} \right\}} \quad \forall i \in CP \quad (19)$$

Total-Value Added (TVA). The *TVA*-value finally describes the economic impact of a given component path flow on the variable process costs (energy, waste and material cost). It is calculated in the following manner

$$TVA^{(c)}_k = MVA^{(c)}_k - EWC^{(c)}_k \quad (20)$$

Usually, only negative *TVA*-values designate process improvement potentials in the process. However, a path flow with an important positive *EWC*-value compensated by an even higher *MVA*-value yields a positive *TVA*-value, but can still bear an energy cost reduction potential.

Stage 3: identification of retrofit options

In this section, the systematic approach for generating retrofit options from the results of the path flow decomposition and assessment procedure is presented. This approach is summarized in Figure 5. In Step 3-1, the component path flows are assigned to five different path flow categories (see Table 1) according to their indicator values as obtained from the path flow assessment procedure. In each category the assigned component path flows are then sorted in ascending order according to their *TVA*-values, which ensures that the path flows are listed in order of economic impact. Because the number of path flows increases considerably as a function of the process complexity (that is, increasing number of supply and demand flows in a process graph), a cut-off *TVA*-value can be defined for practical reasons in order to remove path flows with low economic impact. Yet, this procedure bears the risk that some potential retrofit options are overlooked.

In Step 3-2 important process parameters (later referred to as *optimization parameters*), as well as structural process changes (such as re-piping between existing equipment, replacement of existing equipment, modification and addition of new equipment—later referred to as *structural retrofit alternatives*) are identified that target economic process improvement potentials, as indicated by the economic performance indicators (*MVA*- and *EWC*-indicators). Both optimization parameters and structural alternatives are also referred to as *retrofit options* in the following. To identify these retrofit options, general process actions—formulated in an abstract manner (later referred to as *generic retrofit actions*)—are introduced and used as a check list for each component path flow and path flow category (Table 1). The respective retrofit actions do not comprise any detailed instructions how to actually perform these actions in the context of the investigated process. Realizing a certain retrofit action should result in higher *RQ*- and *TVA*-values. The list of retrofit actions in Table 1 is viewed only as an initial proposition and is not claimed to be complete.

In Step 3-3 all optimization parameters and structural retrofit alternatives that were identified in Step 3-2 are listed, and the cost impact potentials on material and energy costs are calculated. Based on general knowledge of the behavior of process systems, a process engineer can qualitatively judge the effect that a change of an operating parameter or the implementation of a structural retrofit alternative might have on component path flows or unit operations of the process. The process engineer is not required to judge the direction of the effect (such as if temperature is increased in a reactor, is the path flow rate of a product from that reactor going to increase or decrease?). A simple evaluation is only necessary: is the effect on a given component path flow or unit operation expected to be important or negligible? This qualitative evaluation procedure is then used to determine which component path flow(s) and unit-operation(s) are expected to exhibit an important cost sensitivity to a manipulation of a given optimization parameter. The same qualitative evaluation is also carried out in case a structural retrofit alternative is implemented. The costs in both evaluations refer to the *MVA*-value and *EWC*-value in case of component path flows (as calculated in the path flow assessment procedure), and to energy costs in case of unit operations (as given by the energy balance of the base case). This qualitative evaluation is repeated for all retrofit options. It should be noted that this procedure is, of course, highly subject to the user's individual judgement, yet also contributes to a better understanding of

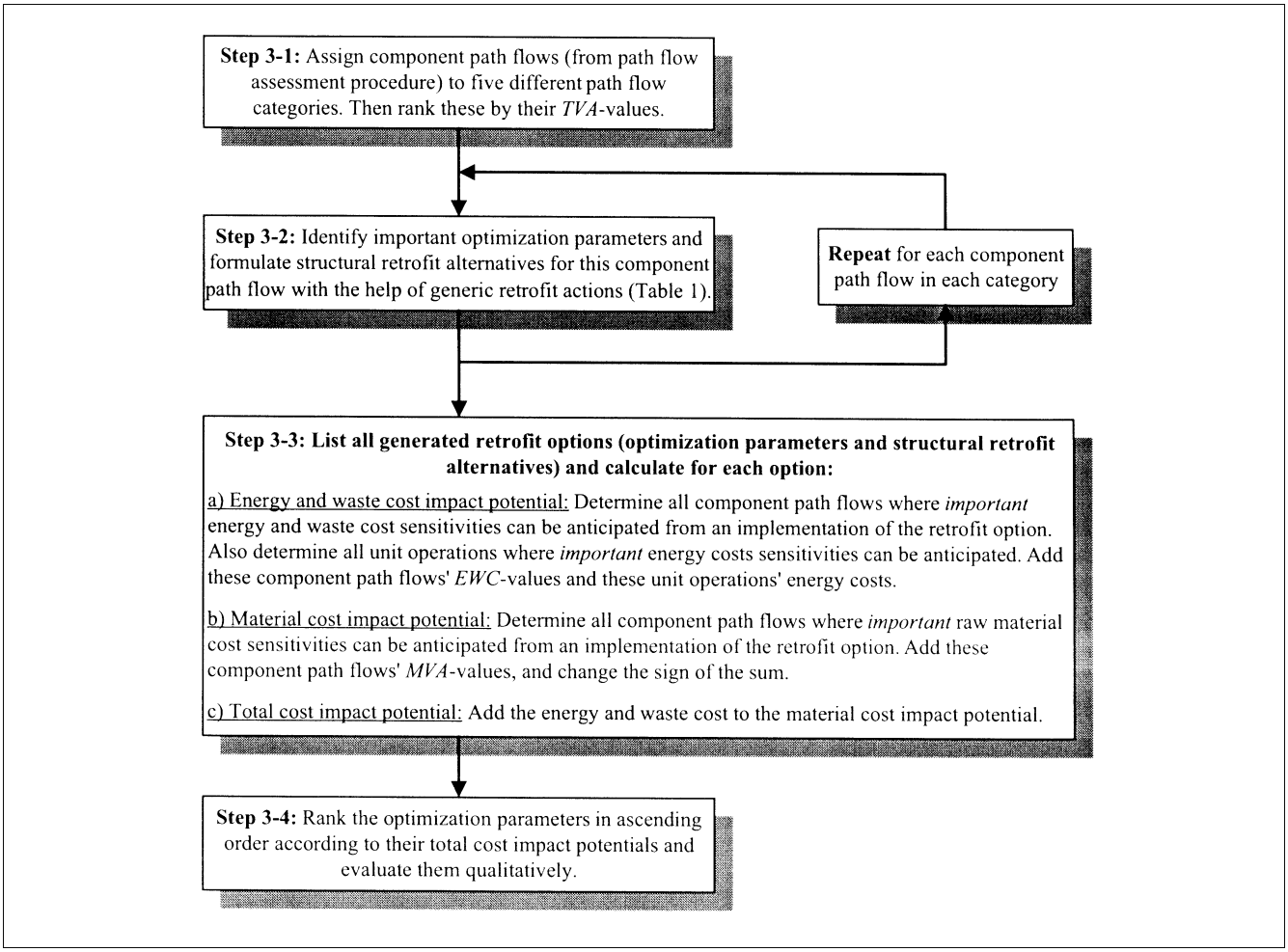

Figure 5. Scheme of Stage 3 of the new method: generating new process alternatives from the results of the assessment procedure (Stage 2).

Table 1. Generic Retrofit Actions for Different Combinations of RQ-, AF-Values and Component Path Flow Types

Component Path Flows	Generic Retrofit Action
All categories	• Reduce the specific energy consumption of the path flow
Category 1 Open component path flows, $RQ \leq 0$	• Reduce/remove the open path flow rate at the source • Reroute (partially) the open path flow in the process • If $RQ = 0$: Recycle (partially) the open path flow to the process only when a positive impact on productivity is expected • Replace the open path flow component with a more suitable component • Increase the specific value $PP_o^{(c)}$ of the open path flow
Category 2 Open component path flows, $RQ > 0$	• Optimize/reduce the open path flow rate • Recycle (partially) the open path flow to the process • Increase the specific value $PP_o^{(c)}$ of the open path flow
Category 3a Cycle component path flows, $RQ \leq 0$, $AF > 1$	• Reduce/remove the cycle path flow rate at the source • Change from a cycle to an open path flow • Reduce the accumulation factor of the cycle path flow • Replace the cycle path flow component with a more suitable component
Category 3b Cycle component path flows, $RQ \leq 0$, $AF \leq 1$	• Reduce/remove the cycle path flow rate at the source • Change from a cycle to an open path flow • Replace the cycle path flow component with a more suitable component • Reroute (partially) the cycle path flow in the process
Category 4 Cycle component path flows, $RQ > 0$	• Optimize the cycle path flow rate • Reroute (partially) the cycle path flow in the process

the cause-effect relationships in the process. Once the qualitative evaluation has been carried out for all retrofit options, the cost impact potentials are calculated for each retrofit option as follows:

- **Energy and Waste Cost Impact Potential:** First, the component path flows that were judged to exhibit an important cost sensitivity with respect to their allocated energy and waste costs are grouped together. Then, the unit-operations that were judged to show an important sensitivity with respect to their energy costs are added to the latter group. The energy and waste cost impact potential for the investigated retrofit option is then calculated by adding the *EWC*-values of these component path flows and the energy costs of these unit operations based on the path flow assessment results.
- **Material Cost Impact Potential:** The material cost impact potential for each retrofit option is calculated in analogy to the energy and waste cost impact potential. The component path flows that were judged to exhibit an important cost sensitivity with respect to their *MVA*-values are grouped together. In order to calculate the material cost impact potential for a given optimization parameter the *MVA*-values of these component path flows have to be added. Since this value is referred to as "material cost impact potential", while it generally exhibits a negative value, the algebraic sign of the calculated sum is switched accordingly.
- **Total Cost Impact Potential:** The total cost impact potential is finally calculated as the sum of the energy and waste cost impact potential and the material cost impact potential for each optimization parameter.

The total cost impact potential, calculated for optimization parameters, is not meant as a cost reduction target, but merely indicates the impact magnitude of the designated parameter on the energy and material costs of the investigated process. More precisely, it indicates the cumulated "leverage effect" or cost effect of each generated optimization parameter on the variable process cost based on the component path flow assessment results. The total cost impact potential is then used to rank the generated optimization parameters relative to each other. The later application of this evaluation to the case study will contribute to a better understanding of the rough evaluation procedure.

The total cost impact potential, calculated for structural retrofit alternatives, equally serves as a rough economic performance indicator to estimate the order of magnitude of the variable cost savings to be expected from the investigated structural retrofit alternative. The interpretation of the meaning of the impact potential for a structural retrofit alternative is different as compared to optimization parameters. This is due to the fact that in the case of structural retrofit alternatives the direction of the effects on component path flows and unit operations can be predicted more easily since these are actually intended to "break" trade-offs in the process. The total cost impact potential can thus be used to rank the different structural retrofit alternatives among each other.

Application to the HDA (Hydro-dealkylation Process for the Production of Toluene) Case Study

The potential of the new methodology is highlighted through its application to a case study, the well-known HDA process reported from open literature.

HDA process description

Douglas (1988) describes various flowsheet alternatives (separation section and plant-wide heat integration alternatives) for the HDA process. Figure 6 shows the flowsheet of

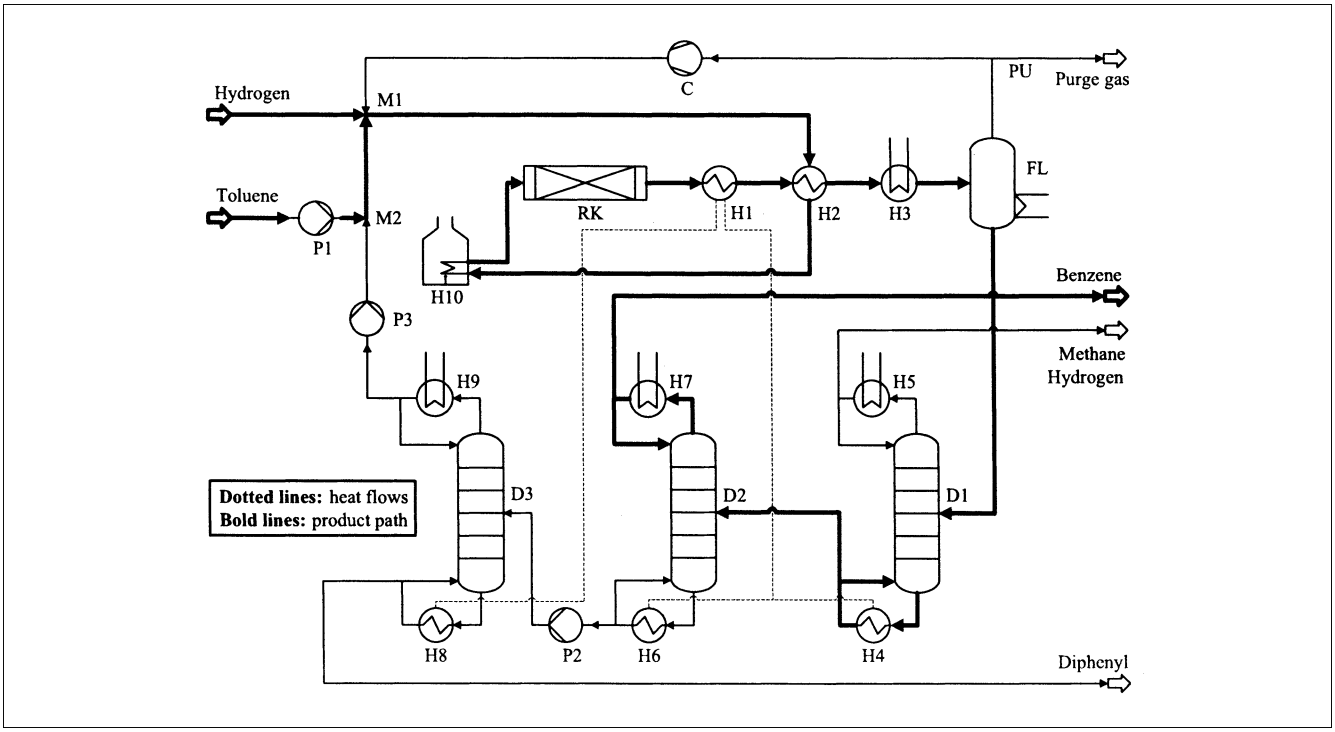

Figure 6. HDA process flowsheet.

the process alternative selected in this article. This specific process alternative corresponds to the HDA alternative that Fisher et al. (1987) used as a base case in their retrofit study and that Kocis and Grossmann (1989) used as initial flowsheet in their MINLP-optimization. The main process operating parameters are also taken from the aforementioned publications such that the results obtained in this article can be compared with those reported in the two earlier studies. The most important design variables are displayed along with the raw material prices, utility costs, and further economic parameters in the Appendix.

Fresh toluene (To) is fed to mixer M2 to which the liquid toluene distillate of column D3 is recycled. Both streams are pumped to the pressure required for reactor RK with pumps P1 and P3. Fresh and already pre-pressurized hydrogen (H_2) with 5 vol. % methane (CH_4) impurity at the desired pressure is then mixed to the toluene stream in mixer M1. Further, the recompressed gas recycle from compressor C that mostly contains methane and hydrogen is also added to the hydrogen/toluene mixture in M1. The resulting hydrogen/toluene/methane mixture is then partially evaporated in heat exchanger H2 and completely evaporated in fired heater H10 before the mixture enters adiabatic reactor RK in which the exothermic main and side reactions to benzene (Bz), methane (CH_4), diphenyl (Dp), and hydrogen occur

$$\mathrm{To} + \mathrm{H_2} \longrightarrow \mathrm{Bz} + \mathrm{CH_4}$$
$$\Delta H_R^{621^\circ\mathrm{C},36\mathrm{bar}} = -49.5\ \mathrm{kJ/mol}, \quad X^{To} = 0.75 \quad (21)$$
$$2\ \mathrm{Bz} \rightleftharpoons \mathrm{Dp} + \mathrm{H_2}$$
$$\Delta H_R^{621^\circ\mathrm{C},36\mathrm{bar}} = 13.0\ \mathrm{kJ/mol}, \quad S^{Dp} = 55 \quad (22)$$

where ΔH_R represents the heat of reaction at the indicated temperature and pressure, X^{To} represents the conversion with respect to toluene, and S^{Dp} represents the selectivity of the formation of diphenyl (defined as the ratio of the benzene molar flow rate to the diphenyl molar flow rate leaving reactor RK).

After the RK reactor outlet is partially condensed (without the noncondensibles hydrogen and methane) in the heat exchange network H1-H4-H6-H8 (process heat is used in the reboilers of the three distillation columns D1, D2, and D3) and in the aforementioned heat exchanger H2, it is further condensed by water quench cooler H3 and then flashed in flash-drum FL. The gas phase that mostly contains the noncondensibles (hydrogen and methane) is then partially purged (PU), recompressed in compressor C, and finally recycled to mixer M1. The liquid phase—containing essentially benzene, diphenyl, and toluene—is processed through stabilizing distillation column D1 to remove the remaining noncondensibles, then through distillation column D2 to separate the desired product benzene, and finally through distillation column D3 to separate byproduct diphenyl from remaining toluene. Recovered toluene with a low diphenyl-concentration is then again recycled to mixer M2. The economic parameters and most important design variables used for the HDA case study are given in the Appendix.

HDA Process Simulation. The HDA process is modeled with the commercial flowsheet software package Aspen Plus$^{\mathrm{R}}$ as a rigorous steady-state simulation. The yearly design production capacity of the simulated HDA process plant is arbitrarily set to 100,000 t (12.5 t/h at 8,000 h operating time). The kinetics for the main reaction and the side reaction were taken from Luyben et al. (1999). The heat integration between the process cooler and the reboilers of the three distillation columns is included in the base case model.

HDA Process Graph. The simplified directed process graph for the HDA case study is shown in Figure 7. For simplification purposes, most of the vertices of the process graph combine multiple unit operations. The fresh hydrogen and toluene feed, pumps P1 and P3, as well as mixers M1 and M2, are represented by vertex MI. The process heat exchange network H1-H4-H6-H8 is combined with process heat exchanger H2, because these heat exchangers require no further utilities. This group of units is represented by two vertices HX1 and HX2 in order to show that no mass exchange actually occurs. The fired heater H10 is then represented as vertex FH and reactor RK as vertex RK. Water quench cooler H3 and flash-drum FL are joined in vertex FL. The three distillation columns D1, D2, and D3, including their condensers H5, H7, and H9, are represented as vertices DS, DB, and DT, respectively. Finally, compressor C is directly represented by vertex CO and purge-split PU by vertex PU.

Results and Discussion

Path flow decomposition and assessment results (Stages 1 and 2, as well as Step 3.1)

Table 2 shows the results of the flow decomposition and assessment procedure applied to the HDA case study. The path flows are sorted according to ascending *TVA*-values in each path flow category. Path flows with highest cost impact potentials appear at the top of each category's list. The Appendix outlines in detail how these results were obtained.

In this case study it is assumed that open path flows O1-O7, O9, O12, O13, and O14 are incinerated and fuel-credit (production of steam) is given for 70% of each component's heat of combustion.

In the first category of Table 2, methane, benzene, and diphenyl open path flows O1-O5 display negative *TVA*-values. No raw-material purchase costs are allocated to methane open path flows O6 and O7, because these are supplied to the process as an impurity in the fresh hydrogen feed. The other methane open path flows O1 and O2 are generated in reactor RK (Figure 7) as a coupled product of the main reaction and account for raw material costs according to Eq. 11. Since methane is a byproduct of the main reaction in reactor RK, but also generates a value outside the system boundaries (fuel-credit), the raw material costs are allocated to benzene, as well as methane, according to Eq. 12. Therefore, methane open path flows O1 and O2 score negative *TVA*-values, as the obtained fuel-credit does not compensate the raw material costs. Open path flow O8 contains the desired product benzene and thus exhibits the highest *TVA*-value of the process. All open path flows of the first category show *RQ*-values of zero. The high *EWC*-value of benzene open path flow O8 is mainly related to its high flow rate.

In contrast to the results in the first category all *TVA*-values for open path flows in the second category are negative. Hydrogen open path flow O9 scores a high negative *TVA*-

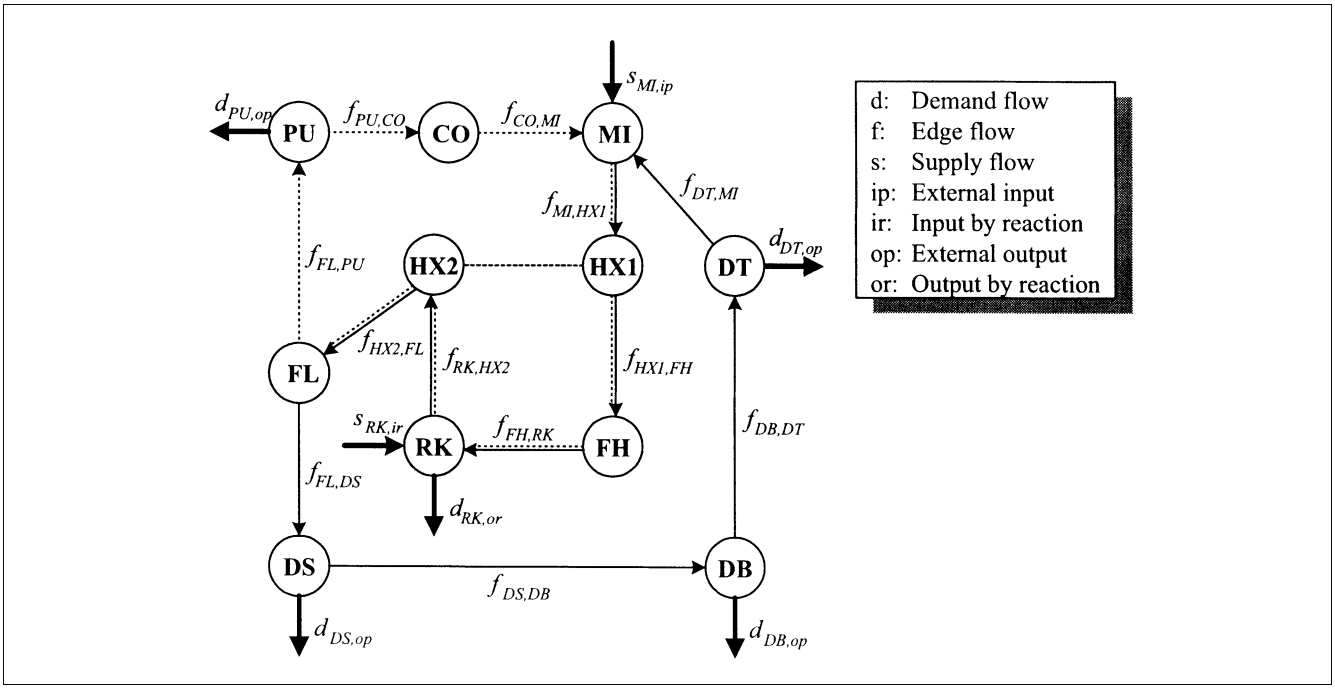

Figure 7. Process graph of the HDA case study.

See text for abbreviations used; dotted arrows: edge flows in the gas cycle; plain arrows: edge flows in the liquid cycle; dotted line between HX1 and HX2: heat flow; -MI-HX1-FH-RK-HX2-FL-DS-DB-: product path; bold arrows: supply and demand flows.

Table 2. Results of Applying Stages 1 and 2, as well as Step 3.1 of the New Method to the HDA Case Study: Component Path Flow Decomposition and Assessment Results

Label	Component	Path*	Mass Flow [kg/h]	*RQ*	*AF*	*EWC* [kU.S.$/a]	*MVA* [kU.S.$/a]	*TVA* [kU.S.$/a]
Category 1: Open path flows, RQ ≤ 0								
O1	CH_4	$s_{RK,ir}$-$d_{PU,op}$	2.56e+3	0	—	7	-11,833	−11,840
O2	CH_4	$s_{RK,ir}$-$d_{DS,op}$	1.20e+2	0	—	1	−553	−554
O3	Bz	$s_{RK,ir}$-$d_{PU,op}$	1.24e+2	0	—	1	−71	−72
O4	Dp	$s_{RK,ir}$-$d_{DT,op}$	3.93e+2	0	—	2	−25	−27
O5	Bz	$s_{RK,ir}$-$d_{DS,op}$	9.00e+0	0	—	4	−5	−9
O6	CH_4	$s_{MI,ip}$-$d_{DS,op}$	1.20e+1	0	—	1	20	19
O7	CH_4	$s_{MI,ip}$-$d_{PU,op}$	2.55e+2	0	—	15	419	404
O8	Bz	$s_{RK,ir}$-$d_{DB,op}$	1.25e+4	0	—	140	19,580	19,440
Category 2: Open path flows, RQ > 0								
O9	H_2	$s_{MI,ip}$-$d_{PU,op}$	3.04e+2	1.06	—	70	−3,660	−3,730
O10	To	$s_{MI,ip}$-$d_{RK,or}$	1.54e+4	1.04	—	554	0	−554
O11	H_2	$s_{MI,ip}$-$d_{RK,or}$	3.31e+2	1.06	—	67	0	−67
O12	H_2	$s_{MI,ip}$-$d_{DS,op}$	3.00e+0	1.06	—	0	−33	−33
O13	To	$s_{MI,ip}$-$d_{PU,op}$	1.60e+1	1.04	—	0	−16	−16
O14	To	$s_{MI,ip}$-$d_{DB,op}$	4.00e+0	1.04	—	1	0	−1
Category 3: Cycle path flows, RQ ≤ 0								
(a) AF > 1								
C1	CH_4	Gas cycle	1.68e+4	0	5.7e0	1,030	0	−1,030
(b) AF ≤ 1								
C2	Bz	Gas cycle	7.42e+2	−0.02	5.8e−2	29	0	−29
C3	Bz	Liquid cycle	1.26e+2	−0.02	9.4e−3	6	0	−6
Category 4: Cycle path flows, RQ > 0								
C4	H_2	Gas cycle	1.82e+3	1.06	5.9e0	459	0	−459
C5	To	Liquid cycle	5.01e+3	1.04	4.4e1	233	0	−233
C6	Dp	Liquid cycle	9.40e+1	0.02	2.4e−1	4	0	−4
C7	To	Gas cycle	9.30e+1	1.04	1.8e−2	4	0	−4

*The abbreviations refer to the vertices of the process graph in Figure 7.

value in the process, almost exclusively because the incineration yields much less value than the original purchase cost. The explanation for the high negative *TVA*-value for toluene open path flow O10 is analogous to the previous discussion on path flow O8. The *RQ*-values in the second category are uniformly above one (only reactant path flows exist in this category).

Methane and hydrogen cycle path flows C1 and C4—both in the gas cycle—score the highest negative *TVA*-values in the third and fourth category of Table 2, respectively. As discussed before, cycle path flows cannot be assessed by the *MVA*-indicator and are, therefore, uniformly set to *MVA*-values of zero. The *TVA*-values then only depend on the generated *EWC*-values. Both cycle path flows C1 and C4 also have similar high *AF*-values, only exceeded by toluene cycle path flow C5. In the third category benzene cycle path flows C2 and C3 show undesirable, slightly negative *RQ*-values while methane cycle path flow C1 essentially acts as an inert component in reactor RK ($RQ = 0$). In the fourth category cycle path flows C4, C5, and C7 have *RQ*-values above one, only diphenyl cycle path flow C6 shows a low positive *RQ*-value of 0.02.

Identification of optimization parameters and structural retrofit options (Step 3.2)

Starting from the assessment results for the HDA process, this section discusses in order of ascending *TVA*-values which generic retrofit actions are found to be applicable to the corresponding component path flows. In this case no cut-off *TVA*-value is chosen for exemplary purposes. After identifying the applicable generic retrofit actions, the most important optimization parameters and/or possible structural retrofit alternatives resulting from these are discussed (see Table 3). The abbreviations for vertices and edge flows of the HDA process in the discussion refer to the notation used in the process graph of Figure 7.

Especially methane open path flow O1 and also O2 display high negative *TVA*-values since these two path flows are generated by the main reaction in reactor RK. These high values follow from the raw material costs that are allocated according to Eq. 12 to both path flows. As methane is a coupled byproduct of the production, the *MVA*-values, which mainly contribute to the high negative *TVA*-values, cannot be influenced without changing the reaction chemistry of the HDA process. This was not considered as a retrofit option in this

Table 3. Results of Applying Step 3.2 of the New Method to the HDA Case Study: Applicable Generic Retrofit Actions and Resulting Optimization Parameters as well as Structural Retrofit Alternatives

Generic Retrofit Action [Path Flow(s)][*]	Optimization Parameters[†] [Label][‡]	Structural Retrofit Alternatives[†] [Label][§]
Hydrogen recycling to the reactor [O9, O12]	—	Introduce a hydrogen/methane separation method [HS1]
Reduction of the accumulation factor of the methane cycle path flow [C1]	Vary the purge in PU while adjusting the hydrogen feed rate to keep the benzene production rate constant [HP1]	Introduce a hydrogen/methane separation method [HS1]
Optimization of the hydrogen path flow rate [C4]	Vary the purge in PU while adjusting the hydrogen feed rate to keep the benzene production rate constant [HP1]	Introduce a hydrogen/methane separation method [HS1]
Optimization of the toluene path flow rate [C5]	Vary the reflux ratio in column DT to vary the toluene recovery in the bottom product and the conversion in reactor RK, while the diphenyl recovery in the distillate is kept constant—adjust the toluene feed rate to the process accordingly [HP2]	—
Better vapor/liquid-separation in vertex FL [O3]	Vary the coolant flow rate in the flash-unit in vertex FL [HP4]	Increase the heat-transfer area in vertex FL [HS2] Use a different utility for vertex FL [HS2]
Diphenyl recycling to the reactor [O4]	Vary the reflux ratio in column DT to vary the diphenyl recovery in the distillate while the toluene recovery in the bottom product is kept constant [HP6]	Bypass the column DT [HS3]
Reduction of the diphenyl open path flow at the source [O4]	Vary the reactor RK pressure [HP5] Vary the reactor RK feed temperature [HP3]	Introduce a more selective catalyst for reactor RK [HS4]

[*]Generic retrofit actions (Table 1) are applied to the component path flow(s) from Table 2.
[†]The abbreviations refer to the vertices of the process graph in Figure 7.
[‡]The labels shown in brackets refer to the optimization parameters given in Table 4.
[§]The labels shown in brackets refer to the structural retrofit alternatives given in Table 5.

article. Methane open path flows O1 and O2 are therefore not taken into account in the process of generating retrofit alternatives.

Hydrogen open path flow O9 displays a high negative *TVA*-value in the investigated HDA process, because the high hydrogen purchase costs largely exceed the fuel credit returned by incineration in $d_{PU,op}$ (Figure 7). Because hydrogen open path flow O9 is assigned to the second category of Table 1 ($RQ = 1.12$), path flow recycling, output value increase, and flow rate optimization or reduction are suggested as possible generic retrofit actions. Assuming that the purge stream has to be incinerated and that the fuel credit cannot be increased, recycling and flow rate optimization of hydrogen path flow O9 are applicable generic retrofit actions. In order to recycle hydrogen open path flows O9, as well as O12 (same situation), a hydrogen/methane separation method (Table 3) is required, as otherwise both components in the purge stream cannot be handled independently from each other. Furthermore, this structural retrofit alternative also signifies a possible way to reduce the accumulation factor of the methane cycle path flow C1 (Table 3) by increased purging without reducing the flow rate of hydrogen cycle path flow C4. Furthermore, the hydrogen/methane separation represents a possibility to optimize the hydrogen path flow rate in C4 (Table 3) independently from the methane cycle path flow C1.

The generic retrofit actions mentioned above can also be performed by varying the appropriate process operating parameters with the exception of hydrogen open path flows O9 and O12 that cannot be recycled to reactor RK by varying operating parameters. The high accumulation factor of the methane cycle path flow C1 can be reduced by increasing purge PU (Figure 7). The same operating parameter can be varied to optimize the flow rate of hydrogen path flow C4. In both cases the hydrogen feed flow rate to the process ($d_{MI,ip}$ in Figure 7) has to be adjusted accordingly.

Toluene cycle path flow C5—listed in the fourth category of Table 2—also shows a high *EWC*-value and a high negative *TVA*-value, accordingly. Since toluene is one of the raw materials of the process, a high accumulation factor is desired in order to recycle it as much as possible. However, optimizing its flow rate might still be a possible generic retrofit action especially as toluene is the limiting reactant in the main reaction of reactor RK (Figure 7). Therefore, optimizing toluene cycle path flow rate in C5 will also affect the conversion in reactor RK. This can be done by varying the toluene recovery in the bottom product of distillation column DT (reflux ratio), while holding the diphenyl recovery in the distillate constant. At the same time, the toluene feed rate to the process in $d_{MI,ip}$ needs to be adjusted to keep the benzene production-rate constant, as highlighted in Table 4. No structural retrofit alternatives are proposed for this generic retrofit action.

Benzene open path flow O3 is due to a non-sharp separation in the flash unit in vertex FL (Figure 7). The path flow displays a negative *TVA*-value in the first category of Table 2. The application of the flow rate reduction action in this category leads to improving the gas-liquid separation efficiency in vertex FL such that the raw material losses induced by purging valuable benzene can be reduced. The benzene flow rate could be reduced by increasing the coolant flow rate (optimization parameter) to the flash unit, as well as the water quench cooler, which could lead to a lower flash outlet temperature and increase the separation efficiency. As structural retrofit alternatives, an increase of the heat-exchange surface in vertex FL (flash unit and water quench cooler) or a lower temperature cooling utility are proposed.

Another savings potential is indicated by the negative *TVA*-value of diphenyl open path flow O4 in the first category of Table 2. Since the side-reaction leading to the formation of diphenyl is reversible, recycling diphenyl open path flow O4 represents an applicable generic retrofit action. Either distillation column DT could be completely by-passed as a structural retrofit alternative, or the diphenyl recovery in the distillate of column DT could be increased by the parameter variation described in Table 4. Alternatively, the generic retrofit action that aims at reducing the diphenyl flow rate in O4 is proposed. This can be performed by either improving the catalyst's selectivity (structural retrofit alternative) or by varying the pressure or the feed temperature of reactor RK (optimization parameters).

The rest of the path flows show only little room for improvement potential and are, therefore, not considered for identifying optimization parameters or structural retrofit alternatives.

Discussion of the identified optimization parameters (Steps 3.3 and 3.4)

The energy and waste cost impact potentials, material cost impact potentials, and total cost impact potentials are calculated for the identified optimization parameters and are displayed in Table 4. This is done by first determining important energy and waste cost sensitive component path flows and important energy cost sensitive unit operations resulting from each variation of an optimization parameter. The *EWC*-values of these component path flows and the energy costs of these unit operations are then added for each optimization parameter. The results are sorted according to the total cost impact potentials in descending order and are discussed in the following.

The variation of the purge (parameter HP1) influences methane and hydrogen open path flow rates C4 and C1 and at the same time requires adjusting of the hydrogen feed rate ($d_{MI,ip}$) to the process in order to keep the production rate of benzene constant. Therefore, parameter HP1 has an impact on cycle path flow rates C1, C4, and hydrogen open path flow rate O9 and, thus, displays by far the highest total cost impact potential among the optimization parameters. However, this parameter is constrained by the fact that the hydrogen/toluene-ratio, which is 8.4 in the base case, may not be decreased below a ratio of 5 (increased coking occurs on the solid-bed catalyst in reactor RK as pointed out by Douglas (1988)).

Parameters HP3, HP5, and HP6 primarily aim at reducing the diphenyl open path flow O4. An increase of the diphenyl recovery in the distillate of column DT (parameter HP6), as explained in Table 4, leads, however, to a higher diphenyl cycle path flow rate in C6 as more diphenyl is recycled. The total cost impact potential is therefore based on diphenyl open path flow O4, diphenyl cycle path flow C6, and the cooling duty needed in the condenser of column DT. Param-

Table 4. Results of Applying Steps 3.3 and 3.4 of the New Method to the HDA Case Study: Total Cost Impact Potentials of the Identified Optimization Parameters

Label	Optimization Parameters from Table 3*	Impact on†	Energy and Waste Cost Impact Potential [kU.S.$/a]	Material Cost Impact Potential [kU.S.$/a]	Total Cost Impact Potential [kU.S.$/a]	Ref.
HP1	Vary the purge in PU while adjusting the hydrogen feed rate to the process	C1, C4, O9	1,560	3,660	5,220	Yes‡
HP2	Vary the reflux ratio in column DT to vary the toluene recovery in the bottom product and the conversion in reactor RK while the diphenyl recovery to the distillate is kept constant—adjust the toluene feed rate to the process accordingly	C4, C5, O9, cooling duty in DT	790	3,660	4,450	Yes‡
HP3	Vary the reactor RK feed temperature (vary furnace FH duty)	O4, furnace duty of FH	2,190	25	2,215	Yes‡
HP4	Vary the coolant flow rate in the flash-unit of vertex FL	O2,§ O3, O5, O6,§ O13, cooling duty of FL	174	92	266	Yes‡
HP5	Vary the reactor RK pressure (vary pressure in compressor CO)	O4, compressor duty of CO	136	25	161	
HP6	Vary the reflux ratio in column DT to vary the diphenyl recovery in the distillate while the toluene recovery in the bottom product is kept constant	O4, C6, cooling duty of DT	35	25	60	Yes‡

*The abbreviations refer to the vertices of the process graph in Figure 7.
†Refers to the important energy and waste cost sensitive component path flows and the important energy cost sensitive unit operations. The component path flow abbreviations refer to Table 2.
‡Fisher et al. (1987).
§Only the *EWC*-value is impacted.

eters HP3 and HP5 on the other hand aim at reducing the diphenyl formation in reactor RK without necessarily impacting the diphenyl cycle path flow rate. Furthermore, parameter HP5 also impacts on the compressor duty in vertex CO and parameter HP3 also impacts on the furnace duty in vertex FH. As the furnace consumes a considerable amount of energy (roughly 8.5 MW), parameter HP3 therefore scores the third highest total cost impact potential. Yet, both feed temperature and pressure in reactor RK can probably not be freely manipulated to improve the selectivity without also affecting the conversion of the main reaction. Also, lowering the pressure too much might be constrained by the desired production capacity for the plant. In turn, increasing the pressure might be constrained by equipment pressure limits.

The variation of the toluene recovery in the bottom product of distillation column DT, as described in Table 4 (parameter HP2), impacts on the flow rate of toluene cycle path C5, as well as on the cooling duty of column DT (not on the heating duty because of heat integration). Since toluene is the limiting reactant in the main reaction of reactor RK, the variation, which scores second priority in Table 4, also impacts on the conversion of this reaction. Therefore, hydrogen cycle path flow C4 and hydrogen open path flow O9 also are impacted. If the toluene recovery is varied, the fresh toluene feed rate to the process has to be adjusted in turn to keep the benzene production rate constant.

Benzene and toluene open path flows O3, O5, and O13 are mainly affected, if the coolant flow rate to the quench and flash unit-operation in vertex FL is varied. The total cost impact potential for this optimization parameter (parameter HP4) does not only take account of these path flows, but also includes the costs for the cooling requirements in that vertex and scores fourth priority in Table 4.

The same HDA process flowsheet was optimized by Fisher et al. (1987). These authors selected the reactor conversion in reactor RK, the purge-split in PU, the furnace-duty in FH,

the coolant flow rate in FL, and the reflux ratio of distillation column DT in a process optimization. A local cost sensitivity analysis was also performed for these parameters and, especially, the conversion and the purge parameter were found to be an order of magnitude more cost-sensitive than the other parameters. The same optimization parameters were also identified by the proposed approach. The results of this approach equally showed that the conversion and purge parameters are by far the most important parameters for a process optimization as they score the highest total cost impact potentials in Table 4.

Discussion of the generated structural retrofit alternatives

The energy and waste cost, material cost, and total cost impact potentials are calculated for the generated structural retrofit alternatives and displayed in Table 5. The results are sorted according to the total cost impact potentials in descending order and discussed in the following.

Alternative HS1 shows by far the most important total cost impact potential in the HDA process among the structural retrofit alternatives. It aims at reducing the *EWC*- and *MVA*-values of hydrogen open path flow O9, O12, and methane cycle path flow C1. Yet, the technical feasibility of a hydrogen/methane-separation method must be analyzed and the attainable cost savings potential assessed accordingly. Although large investment costs are to be expected, the total cost impact potential still indicates a fair chance for a good return on investment. Kocis and Grossmann (1989) formulated a MINLP-optimization for the same HDA process and found that the proposed hydrogen/methane-separation method (membrane separation) was part of the final optimal flowsheet structure. This fact supports the assignment of the highest cost impact potential to alternative HS1, as done by the method proposed here.

Both options proposed with alternative HS2 (that is, the increase of the heat-transfer area and the use of chilled water in vertex FL) aim at reducing the *EWC*- and *MVA*-values of benzene and toluene open path flows O3, O5, and O13. At the same time, methane open path flows O6 and O7 will be partially rerouted from the stabilizing column DS (Figure 7) to gas-cycle purge PU and thus reduce energy costs for cooling in the condenser of that column. Yet, the total cost impact potential for alternative HS2 is probably not high enough to justify an investment for increasing the heat-transfer area. Therefore, the best option would be to optimize the cooling duty with the presently used coolant as previously discussed. Only if the cost-optimal cooling duty is higher than the cooling capacity of the quench- and flash-unit in vertex FL, a change to a colder coolant (such as chilled water) might be considered.

Bypassing distillation column DT (alternative HS3) offers a complete recycling of diphenyl without any related investment costs, yet generates additional energy costs because diphenyl will consequently accumulate in the liquid cycle path to a level where the reversible formation of diphenyl reaches a thermodynamic equilibrium. The total cost impact potential (third highest potential in Table 5), therefore, results from the *EWC*- and *MVA*-values of diphenyl open path flow O4 and from the cooling duty requirement in distillation column DT.

Finally, alternative HS4, which also aims on reducing the *EWC*- and *MVA*-values of diphenyl path flow O4, requires investment costs for further catalyst research and will most likely not yield a complete reduction of the diphenyl formation in reactor RK. Because of the research costs and the lower total cost impact potential, it can in this case be concluded that alternative HS3 is preferable to alternative HS4.

In principle, the process improvements through alternatives HS1, HS2 and either HS3 or HS4 can all be carried out

Table 5. Results of Applying Steps 3.3 and 3.4 of the New Method to the HDA Case Study: Total Cost Impact Potentials of the Generated Structural Retrofit Alternatives

Label	Structural Retrofit Alternatives from Table 3*	Impact on†	Energy and Waste Cost Impact Potential [kU.S.$/a]	Material Cost Impact Potential [kU.S.$/a]	Total Cost Impact Potential [kU.S.$/a]	Ref.
HS1	Introduce a hydrogen/methane separation method	O9, O12, C1	1,100	3,690	4,790	Yes‡
HS2	Increase the heat-transfer area in vertex FL Use chilled water for vertex FL	O2,‖ O3, O5, O6,‖ O13, cooling duty of FL	174	92	266	Yes§
HS3	Bypass column DT	O4, cooling duty of DT	31	25	56	—
HS4	Introduce a more selective catalyst in reactor RK	O4	2	25	27	—

*The abbreviations refer to the vertices of the process graph in Figure 7.
†The component path flow abbreviations refer to Table 2.
‡Kocis and Grossmann (1989).
§Fisher et al. (1987).
‖Only the *EWC*-value is impacted.

simultaneously. Of course, the attainable total cost savings potentials need to be determined in a detailed study (such as rigorous simulation) and must be checked on their technical feasibility. However, this study is not performed in this article.

Conclusions

This article has presented a new methodology for screening the cost-savings potentials of continuous chemical processes. The method systematically decomposes the flowsheet of the investigated process into open and cycle component path flows and allocates the variable process costs to these path flows. Besides the economic parameters, additional indicators are also used to characterize the degree of nonideality of each path flow. These indicators are then used to formulate retrofit options and to rank these according to their cost-impact potential. The method was applied to the HDA case study and highlighted several promising retrofit options that were discussed in regard to their technical feasibility. The results obtained demonstrate how the systematic framework of the new methodology supports the identification of economically beneficial retrofit options for chemical processes. Similar conclusions were drawn from the application of the method to a complex industrial case study that will be discussed in a followup article (together with additional stages of the overall approach).

Once a process flowsheet with the required mass- and energy balances is available for the process under investigation, the method can be quickly carried out and the results easily communicated. A Microsoft Excel program has been developed that automatically does the decomposition and assessment after the flow rates have been copied into a corresponding sheet. This helps considerably in quickly applying the method in daily practice. However, since a process generally behaves in a nonlinear fashion, the calculated total savings potential of a generated retrofit option should be only viewed as an order-of-magnitude estimate. The attainable cost savings for a given retrofit option still needs to be determined using rigorous calculations. The presented methodology has been specifically developed for retrofit design and, due to its modular nature, could be modified to accommodate additional retrofit goals such as reducing process emissions to the environment or increasing production capacity. As the screening method generates potentially attractive retrofit options, this method could also be used to systematically identify and focus on the most promising structural elements for a MINLP-superstructure.

Acknowledgment

The authors thank two anonymous reviewers for their detailed and constructive comments that helped to improve the manuscript.

Notation

A = energy allocation factor (see Appendix)
AF = accumulation factor indicator
$\overline{B}$ = edge-vertex incidence matrix of the sub-graph, (dimensions: edges $*$ vertices)
CA = cost allocation factor
$\vec{d}$ = vertices total demand flow rate vector of the sub-graph, kg/h
d = vertex demand flow rate, kg/h
$\overline{D}$ = cycle-edge incidence matrix, (dimensions: cycles $*$ edges)
E = effect of a component path flow on a reaction rk
EC = energy cost indicator, US$/a
EWC = energy and waste cost indicator, US$/a
$\vec{f}$ = edge flow rate vector of the complete process graph, kg/h
f = edge flow rate, kg/h
F = sum of input mass flow rates to a vertex, kg/h
M = molecular weight, kg/kmol
MVA = material-value added indicator, US$/a
m = component path flow rate, kg/h
n = molar flow rate, mol/h
p = pressure, Pa
PE = price of a utility, US$/MJ
PP = specific value of a path flow, US$/kg
PR = price of a raw material, US$/kg
ρ = density, kg/m^3
Q = energy consumption of a sub-operation, kW
RQ = reaction quality indicator
$\vec{s}$ = vertices total supply flow rate vector of the sub-graph, kg/h
s = vertex supply flow rate, kg/h
T = temperature, K
TVA = total value added indicator, US$/a
V = volumetric flow rate, m^3/h
w = flow distribution factor
WAC = concentration-specific waste-allocation factor, US$ m^3/kg
WAM = mass-specific waste-allocation factor, US$/kg
WAV = volume-specific waste-allocation factor, US$/m^3
WC = waste treatment cost, US$/a
$\vec{x}$ = vector of maximum component cycle flow rates, kg/h
$\vec{y}$ = vector of component path flow rate fractions
y = component edge flow rate fraction
ν = stoichiometric coefficient
ξ = reaction extent of a reaction, mol/h

Subscripts

a = index of edges positively incident with a vertex, {1, …, EP}
b = index of edges negatively incident with a vertex, {1, …, EN}
fp = index of desired products of the process, {1,…, FP}
i = index of vertices, {1, …, I}
ip = index of feed flows (non-edge flows) to a vertex, {1, …, IP}
ir = index of supply flows due to reaction in a vertex, {1, …, IR}
j = index of edges leaving the process boundaries, {1, …, J}
k = index of cycle and open path flows of a component, {1, …, K}
o = index of open path flows of a component, {1, …, O}
op = index of output flows (non-edge flows) from a vertex, {1, …, OP}
or = index of demand flows due to reaction in a vertex, {1, …, OR}
pd = index of products generated in a gross reaction equation, {1, …, PD}
r = index of reactive unit-operations of a component path flow, {1, …, R}
rk = index of reactions in reactive unit-operation r affected by component path flow k, {1, …, RK}
m = arithmetic mean value (input and output of a sub-operation)
u = index of sub-operations along a component path flow, {1, …, U}
uk = index of component path flows involved in a sub-operation, {1, …, UK}
z = index of cycle path flows, {1, …, Z}

Superscripts

c = component index
rm = index of raw materials involved in gross reaction scheme to generate component c, {1, …, RM}

Mathematical operators

diag = diagonalization of a vector

Sets

CP = set of vertices forming a cycle path
SC = set of components flowing in the sub-graph
SG = set of all sub-graph vertices

Literature Cited

Ciric, A. R., and C. A. Floudas, "A Retrofit Approach for Heat Exchanger Networks," *Comp. Chem. Eng.*, **13**, 703 (1989).

Dantus, M. M., and K. A. High, "Economic Evaluation for the Retrofit of Chemical Processes through Waste Minimization and Process Integration," *Ind. Eng. Chem. Res.*, **35**, 4566 (1996).

Douglas, J. M., "Hierarchical Decision Procedure for Process Synthesis," *AIChE J.*, **31**, 353 (1985).

Douglas, J. M., *Conceptual Design of Chemical Processes*, McGraw-Hill, New York (1988).

Fisher, W. R., M. F. Doherty, and J. M. Douglas, "Screening of Process Retrofit Alternatives," *Ind. Eng. Chem. Res.*, **26**, 2195 (1987).

Fraser, D. M., and N. Hallale, "Retrofit of Mass Exchange Networks Using Pinch Technology," *AIChE J.*, **45**, 2112 (2000).

Guntern, C., A. H. Keller, and K. Hungerbühler, "Economic Optimization of an Industrial Semibatch Reactor Applying Dynamic Programming," *Ind. Eng. Chem. Res.*, **37**, 4017 (1998).

Jaksland, C., R. Gani, and K. Lien, "Separation Process Design and Synthesis Based on Thermodynamic Insights," *Chem. Eng. Sci.*, **50**, 511 (1995).

Kocis, G. R., and I. E. Grossmann, "A Modelling and Decomposition Strategy for the MINLP Optimization of Process Flowsheets," *Comp. Chem. Eng.*, **13**, 797 (1989).

Kovac, A., and C. Glavic, "Retrofit of Complex and Energy Intensive Processes I," *Comp. Chem. Eng.*, **19**, 1255 (1995).

Kürum, S., E. Heinzle, and K. Hungerbühler, "Plant Optimisation by Retrofitting Using a Hierarchical Method: Entrainer Selection, Recycling and Heat Integration," *J. Chem. Biotechnol.*, **70**, 29 (1997).

Linnhoff, B., and J. R. Flower, "Synthesis of Heat-Exchanger Networks. 1. Systematic Generation of Energy Optimal Networks," *AIChE J.*, **24**, 633 (1978).

Luyben, W. L., B. D. Tyreus, and M. L. Luyben, *Plantwide Process Control*, McGraw-Hill, New York (1999).

Rapoport, H., R. Lavie, and E. Kehat, "Retrofit Design of New Units into an Existing Plant: Cast Study: Adding New Units to an Aromatics Plant," *Comp. Chem. Eng.*, **18**, 743 (1994).

Sargent, R. W. H., and A. W. Westerberg, "'Speed-Up' in Chemical Engineering Design," *Trans. Inst. Chem. Engrs.*, **42**, T190 (1964).

Tarjan, R., "Depth-First Search and Linear Graph Algorithms," *SIAM J. Comput.*, **1**, 147 (1972).

Tjoe, T. N., and B. Linnhoff, "Using Pinch Technology for Process Retrofit," *Chem. Eng.*, **93**, 47 (1986).

Van der Helm, D. U., and K. A. High, "Waste Minimization by Process Modifications," *Environ. Prog.*, **15**, 56 (1996).

Appendix A

This section demonstrates the path flow decomposition and assessment procedure as described in the article using benzene in the HDA process as an example.

Path flow decomposition (Steps 1-1 to 1-4): example benzene

In the HDA process all vertices of the complete process graph are also part of the sub-graph. In Step 1-1, two cycles are identified (see Figure 6): a gas-cycle (dotted path) and a liquid-cycle (plain path) for which the incidence matrix $\overline{B}^{Bz}$

Table A1. Flow Distribution Factors for Benzene in the HDA Process

	$f_{MI,HX1}$	$f_{HX1,FH}$	$f_{FH,RK}$	$f_{RK,HX2}$	$f_{HX2,FL}$	$f_{FL,PU}$	$f_{PU,CO}$	$f_{CO,MI}$	$f_{FL,DS}$	$f_{DS,DB}$	$f_{DB,DT}$	$f_{DT,MI}$	$s_{RK,ir}$	$d_{PU,op}$	$d_{DS,op}$	$d_{DB,op}$
MI	0	0	0	0	0	0	0	0	0	0	0	0	0	0	0	0
HX1	0	0	0	0	0	0	0	0	0	0	0	0	0	0	0	0
FH	0	0	0	0	0	0	0	0	0	0	0	0	0	0	0	0
RK	0	0	0	1	0	0	0	0	0	0	0	0	0	0	0	0
HX2	0	0	0	0	1	0	0	0	0	0	0	0	0	0	0	0
FL	0	0	0	0	0	0.0098	0	0	0.9902	0	0	0	0	0	0	0
PU	0	0	0	0	0	0	0	0	0	0	0	0	0	1	0	0
CO	0	0	0	0	0	0	0	0	0	0	0	0	0	0	0	0
DS	0	0	0	0	0	0	0	0	0	0.99925	0	0	0	0	0.00075	0
DB	0	0	0	0	0	0	0	0	0	0	0	0	0	0	0	1
DT	0	0	0	0	0	0	0	0	0	0	0	0	0	0	0	0

Table A2. Mass-Flow Rates Obtained for Benzene in the HDA Process by Applying the Path Flow Decomposition Procedure

k	Benzene Path Flow	m_k^{Bz}, [kg/h]
1	Gas-cycle (dotted path in Figure 6)	742
2	Liquid-cycle (plain path in Figure 6)	126
3	$s_{RK,ir} - f_{RK,\ HX2} - f_{HX2,FL} - f_{FL,DS} - f_{DS,DB} - d_{DB,op}$	12,500
4	$s_{RK,ir} - f_{RK,HX2} - f_{HX2,FL} - f_{FL,DS} - d_{DS,op}$	9
5	$s_{RK,ir} - f_{RK,HX2} - f_{HX2,FL} - f_{FL,PU} - d_{PU,op}$	124

is formulated as

$$\bar{B}^{Bz} = \begin{pmatrix} 1 & 0 & 0 & 0 & 0 & 0 & 0 & -1 & 0 & 0 & 0 & -1 \\ -1 & 1 & 0 & 0 & 0 & 0 & 0 & 0 & 0 & 0 & 0 & 0 \\ 0 & -1 & 1 & 0 & 0 & 0 & 0 & 0 & 0 & 0 & 0 & 0 \\ 0 & 0 & -1 & 1 & 0 & 0 & 0 & 0 & 0 & 0 & 0 & 0 \\ 0 & 0 & 0 & -1 & 1 & 0 & 0 & 0 & 0 & 0 & 0 & 0 \\ 0 & 0 & 0 & 0 & -1 & 1 & 0 & 0 & 1 & 0 & 0 & 0 \\ 0 & 0 & 0 & 0 & 0 & -1 & 1 & 0 & 0 & 0 & 0 & 0 \\ 0 & 0 & 0 & 0 & 0 & 0 & -1 & 1 & 0 & 0 & 0 & 0 \\ 0 & 0 & 0 & 0 & 0 & 0 & 0 & 0 & -1 & 1 & 0 & 0 \\ 0 & 0 & 0 & 0 & 0 & 0 & 0 & 0 & 0 & -1 & 1 & 0 \\ 0 & 0 & 0 & 0 & 0 & 0 & 0 & 0 & 0 & 0 & -1 & 1 \end{pmatrix} \quad \text{(A1)}$$

where the rows and columns represent vertices and edges respectively:

- *Rows:* MI, HX1, FH, RK, HX2, FL, PU, CO, DS, DB, DT
- *Columns*: $f_{M1,HX1}$, $f_{HX1,FH}$, $f_{FH,RK}$, $f_{RK,HX2}$, $f_{HX2,FL}$, $f_{FL,PU}$, $f_{PU,CO}$, $f_{CO,MI}$, $f_{FL,DS}$, $f_{DS,DB}$, $f_{DB,DT}$, $f_{DT,MI}$

Along with the edge, supply, and demand flow-rate vectors (units: kg/h)

$$\vec{f}^{Bz} = \begin{pmatrix} 868 \\ 868 \\ 868 \\ 13500 \\ 13500 \\ 866 \\ 742 \\ 742 \\ 12630 \\ 12630 \\ 126 \\ 126 \end{pmatrix}, \vec{s}^{Bz} = \begin{pmatrix} 0 \\ 0 \\ 0 \\ 12630 \\ 0 \\ 0 \\ 0 \\ 0 \\ 0 \\ 0 \\ 0 \\ 0 \end{pmatrix}, \vec{d}^{Bz} = \begin{pmatrix} 0 \\ 0 \\ 0 \\ 0 \\ 0 \\ 0 \\ 124 \\ 0 \\ 9 \\ 0 \\ 12500 \end{pmatrix} \quad \text{(A2a–c)}$$

the mass-balance equation system is established in Step 1-2 using Eqs. 1–3.

The solution of the optimization problem (Eqs. 5 and 6) yields the vector containing the maximum edge flow rates circulating in both cycles

$$\text{diag}\left(\vec{f}^{Bz}\right)\vec{y}^{Bz} = \text{diag}\begin{pmatrix} 868 \\ 868 \\ 868 \\ 13500 \\ 13500 \\ 866 \\ 742 \\ 742 \\ 12630 \\ 12630 \\ 126 \\ 126 \end{pmatrix}\begin{pmatrix} 1 \\ 1 \\ 1 \\ 0.064 \\ 0.064 \\ 1.167 \\ 1 \\ 1 \\ 0.001 \\ 0.001 \\ 1 \\ 1 \end{pmatrix} = \begin{pmatrix} 868 \\ 868 \\ 868 \\ 868 \\ 868 \\ 742 \\ 742 \\ 742 \\ 126 \\ 126 \\ 126 \\ 126 \end{pmatrix} \quad \text{(A3)}$$

Table A3. Economic Values Used in the Calculation of the *MVA*-Indicator for Benzene Path Flows in the HDA Process

k	PR_k^{To}, [U.S.$/kg]	PR_k^{H2}, [U.S.$/kg]	PP_k^{Bz}, [U.S.$/kg]	PP^{CH_4}, [U.S.$/kg]	VA_k^{Bz}, [kU.S.$/a]
3	0.3	2.0	0.44 (sales)	0.21 (fuel)	19,600
5	0.3	2.0	0.17 (fuel)	0.21 (fuel)	−72

Table A4. Energy Cost Allocation for Benzene Path Flows in the HDA Process

Vertex Sub-op. u	FH Heater Heating	FL Quench Cooling	FL Flash Cooling	FL Flash Condensing	CO Compressor Compressing
Utility	Natural Gas	Cool. Water	Cool. Water	Cool. Water	Electricity
Q_u, [kW]	8,680	561	3,480*	2,010*	356
PE_u, [U.S.$/GJ]	8.8†	1.0‡	1.0‡	1.0‡	13.1
	Capacity				
A_u	Heat (g)	Heat (g)	Heat (g)	Heat of Vapor (Bz, To & Dp)	Molar Vol. (g)
T_m, [K]	522	163	96	96	48
p_m, [MPa]	3.8	3.4	3.3	3.3	3.6
Total Flow Rates [kg/s]					
Bz	868	13,500	13,500	13,500	742
To	20,500	5,120	5,120	5,120	93
H_2	2,450	2,120	2,120	2,120	1,820
Dp	94	487	487	487	0
CH_4	17,100	19,700	19,700	19,700	16,800
$EC_{k,1}^{Bz}$, [kU.S.$/a]	**25.0**	**0.2**	**0.9**	**2.2**	**0.6**

*The total energy consumption for the flash operation (5,490 kW) is attributed to two sub-operations: cooling and condensing.
†Assumes 80% efficiency in the furnace.
‡Assumes an average temperature rise in the cooling water of 5°C after cooling.

Table A5. Parameters Used for the Calculation of the *RQ*-Indicator for Benzene Path Flows in the HDA Process

k	$E^{Bz}_{R1,RK,k}$	$E^{Bz}_{2,RK,k}$	$\xi_{R1,RK}$ [kmol/h]	$\xi_{R2,RK}$ [kmol/h]	$n^{(Prod)}$ [kmol/h]	RQ^{Bz}_k
1	0	−1	167	2.6	160	−0.02
2	0	−1	167	2.6	160	−0.02

Table A6. Accumulation Factors Calculated for Path Flows in Table A5

k	m^{Bz}_k [kg/h]	Sum of Output Flows [kg/h]	AF^{Bz}_k
1	742	12,800	0.06
2	126	13,400	0.01

Furthermore, the over-determined equation system (Eq. 7) is set up with the use of $\overline{D}^{Bz}$ (left column: edges in gas-cycle; right column: edges in liquid-cycle)

$$\overline{D}^{Bz} = \begin{Bmatrix} 11 \\ 11 \\ 11 \\ 11 \\ 11 \\ 10 \\ 10 \\ 10 \\ 01 \\ 01 \\ 01 \\ 01 \end{Bmatrix} \tag{A4}$$

and results in the maximal cycle path flows $\vec{x}^{Bz}$: gas-cycle: 742 kg/h; liquid-cycle: 126 kg/h.

In Step 1-3 the cycle path flows are subtracted from the original edge flow rates in the sub-graph and the flow distribution factors are calculated in Step 1-4 (Table A1).

Finally, Table A2 shows the results of the complete decomposition procedure for benzene.

Component path flow assessment (Stage 2): selected benzene path flows (Table A2)

MVA-values for path flows 3 & 5. It is assumed that the purge stream $d_{PU,op}$ is incinerated and fuel credit for 70% of the combustion enthalpy is given. The overall reaction equation for the formation of benzene from raw materials toluene and hydrogen corresponds to the main reaction. The results are shown in Table A3.

EWC-value for path flow 1. The benzene gas-cycle path flow causes utility consumption in the fired heater FH, the quench and flash operations in FL, and the compressor CO. All other vertices involved in the gas cycle do not consume utilities with respect to benzene (reactor in RK operates in

Table B1. Economic Parameters and Important Design Variables for the HDA Case Study*

Feedstock/product	Comment	Price [U.S.$/kg]
H_2-feed	95 mol % H_2, 5 mol% CH_4, 38 bar 38 bar	2.00
To-feed	100% To, 1 atm	0.30
Bz-product	99.97 wt. % Bz	0.44
Utilities	**Comment**	**Costs**
Natural gas		0.025 U.S.$/kWh
Electricity		0.047 U.S.$/kWh
Cooling water		0.1 U.S.$/m3
Chilled water		0.1 U.S.$/m3
Steam	Produced by waste incineration	12 U.S.$/t
Most Important Design Variables		
Plant design capacity		100,000 t/a
Reactor (RK)	Temperature (in, out)	894, 943 K
	Average pressure	36 bar
	H_2/To molar ratio	5.5
Fired heater (FH)	Heating duty	8.8 MW
Quench & flash-drum	Cooling duty	6 MW
Flash-drum (FL)	Temperature	38°C
	Pressure	33 bar
Purge stream (PU)	H_2 molar fraction	0.46
Stabilizing column (DS)	Reflux ratio	1
	Pressure	10 bar
	No. Stages	25
Benzene column (DB)	Reflux ratio	1.3
	Pressure	1 atm
	No. Stages	55
Toluene column (DT)	Reflux ratio	1.0
	Pressure	1 atm
	No. Stages	20

*See article for Abbreviations Used.

adiabatic mode, HX1-HX2 exchanges process heat, PU does not consume utilities, and MI only needs electricity for toluene pumping). The gas cycle does not undergo waste treatment—therefore, only energy costs have to be allocated. The calculation and the result of the *EWC*-value are shown in Table A4.

RQ-values for path flows 1 & 2. *RQ*-values can be assigned only to the benzene gas- and liquid-cycle path flows because the remaining open benzene path flows do not affect the only reactive unit-operation (vertex RK) in the flowsheet. The recycling of benzene has a negative effect on overall benzene productivity due to the equilibrium side-reaction to diphenyl. Both path flows yield the same results shown in Table A5.

AF-values for path flows 1 & 2. The benzene gas-cycle path flow has flows $f_{FL,DS}$, $d_{RK,or}$, and $d_{PU,op}$ (see Figure 6) leaving the cycle path, while flows $f_{FL,PU}$, $d_{DS,op}$, $d_{DB,op}$, and $d_{DT,op}$ leave the liquid-cycle path flow. The corresponding *AF*-values are calculated as illustrated in Table A6.

Appendix B

Table B1 displays the economic parameters and the most important design variables used for the HDA case study.

Manuscript received Sept. 13, 2002, and revision received Feb. 26, 2003.